

## Dense $\beta$ -SiAlONs consolidated by a modified hydrolysis-assisted solidification route

Ibram Ganesh<sup>a,b</sup>, N. Thiyagarajan<sup>a</sup>, D.C. Jana<sup>a</sup>, P. Barick<sup>a</sup>,  
G. Sundararajan<sup>a</sup>, J.M.F. Ferreira<sup>b,\*</sup>

<sup>a</sup> Centre for Silicon Carbide, International Advanced Research Centre for Powder Metallurgy and New Materials (ARCI), Hyderabad 500005, AP, India

<sup>b</sup> Department of Ceramics and Glass Engineering, CICECO, University of Aveiro, Aveiro P-3810193, Portugal

Received 23 May 2007; received in revised form 24 July 2007; accepted 5 August 2007

Available online 23 October 2007

### Abstract

Dense  $\beta$ -Si<sub>4</sub>Al<sub>2</sub>O<sub>2</sub>N<sub>6</sub> materials were fabricated by a modified hydrolysis-assisted solidification (HAS) route from aqueous slurries containing 48–50 vol.% solids, in which 5–22 wt.% of the required  $\alpha$ -Al<sub>2</sub>O<sub>3</sub> was replaced by equivalent amounts of unprotected aluminium nitride (AlN) powder to promote consolidation *via* AlN hydrolysis. A fixed amount (9.37 wt.%) of AlN passivated against hydrolysis with a coating phosphate layer was also added to all the samples consolidated by the modified HAS method. The aqueous slurries were cast in non-porous moulds, allowed to set and dried before sintering at 1675 °C for 4 h. For comparison purposes, ceramics with the same predicted final composition (having 64.33%  $\alpha$ -Si<sub>3</sub>N<sub>4</sub>, 23.36%  $\alpha$ -Al<sub>2</sub>O<sub>3</sub>, 9.37% AlN and 7% Y<sub>2</sub>O<sub>3</sub> as starting materials) were also consolidated by a conventional dry-powder pressing (CDPP). The  $\beta$ -Si<sub>4</sub>Al<sub>2</sub>O<sub>2</sub>N<sub>6</sub> ceramics consolidated by the modified HAS route exhibited superior outstanding properties (bulk density, apparent porosity, water absorption capacity, hardness and fracture toughness) in comparison to the traditional dry-powder pressing route.

© 2007 Elsevier Ltd. All rights reserved.

**Keywords:** Si<sub>4</sub>Al<sub>2</sub>O<sub>2</sub>N<sub>6</sub>; Hydrolysis-assisted solidification; Reaction sintering; Y<sub>2</sub>O<sub>3</sub>; Thermal expansion

### 1. Introduction

Recently,  $\beta$ -SiAlON ceramics have been considered as potential candidate materials for many commercially important applications.<sup>1–5</sup> These ceramics are normally made by a conventional dry-powder pressing technique followed by reaction sintering of precursor mixtures at elevated temperatures to achieve full density, followed by extensive and expensive machining to obtain the desired shape.<sup>6,7</sup> However, this technique has been found to be difficult and quite expensive particularly for making large size and complex shaped components. In order to make components with high density and high uniformity, and thus, high reliability of performance, a great variety of aqueous based colloidal forming techniques such as, slip casting,<sup>8</sup> tape casting,<sup>9</sup> gelcasting,<sup>10,11</sup> temperature-induced forming process,<sup>12</sup> hydrolysis-assisted solidification (HAS),<sup>13–15</sup> etc., have been developed recently. Among these

techniques, aqueous gelcasting was found to be one of the most effective routes for making near net-shape parts with relatively high green strength.<sup>16</sup> However, as the organic monomers used in this process are very expensive, this process is not viable for making many of the commercially important products to be fabricated in large quantity.<sup>14,15</sup> Further, as the forming technique impacts directly the productivity, the ultimate quality and the cost of the manufactured products, in the case of mass productions of several advanced ceramics, high productivity with minimum cost must be fulfilled. In view of these reasons, there is still an open quest for the development of ever cheaper routes for processing of these ceramic materials.

Hydrolysis-assisted solidification (HAS) is a very simple and economic net-shaping process that has been used to consolidate several kinds of ceramics like Si<sub>3</sub>N<sub>4</sub>,<sup>13</sup> ZTA,<sup>14</sup> SiC,<sup>15</sup> etc., in which alumina can be a minor or major phase.<sup>14,15</sup> This process does not require expensive tools nor complex procedures. Further, it is less demanding in terms of the starting solids loading of the suspensions (above ca. 30 vol.%) in comparison to gelcasting that requires a high solids content, and the starting pH of the suspensions can vary from moderate acid to alkaline.<sup>14,15</sup> In the

\* Corresponding author. Tel.: +351 234 370242; fax: +351 234 425300.  
E-mail address: [jmf@cv.ua.pt](mailto:jmf@cv.ua.pt) (J.M.F. Ferreira).

HAS process, the consolidation takes place due to the hydrolysis of aluminium-nitride powder, which causes dramatic increases in the viscosity of the ceramic suspension leading to its consolidation. Several mechanisms such as, flocculation/coagulation induced by the pH change of the suspension towards the IEP of the ceramic powder, gelling of  $\text{Al}(\text{OH})_3$  reaction product and forming a stiff network, consuming of water during the formation of  $\text{AlOOH}$  and  $\text{Al}(\text{OH})_3$ , etc., are involved in this consolidation process. Among all these mechanisms, the ultimate green strength of the consolidated part is mainly influenced by the amount of  $\text{Al}(\text{OH})_3$  network formed by the hydrolysis of  $\text{AlN}$  powder. As this process is associated with the evolution of  $\text{NH}_3$  gas ( $\text{AlN} + 2\text{H}_2\text{O} \rightarrow \text{AlOOH} + \text{NH}_3$ ), it is always a difficult task to fix the desired amount of  $\text{AlN}$  required to obtain a green body with sufficient green strength and without any un-desired porosity.

As  $\beta\text{-Si}_{6-z}\text{Al}_z\text{O}_z\text{N}_{6-z}$  with  $z=2$  has been identified as a potential candidate material for certain radome applications,<sup>10,11</sup> a systematic investigation was conducted to study the ability of a modified hydrolysis-assisted solidification process for fabrication of ceramic components out of this composition. The ceramics made by this new process were sintered at  $1675^\circ\text{C}$  for 4 h under  $\sim 800$  Torr  $\text{N}_2$  pressure along with those obtained by the conventional dry-powder pressing (CDPP) route. The sintered materials were thoroughly characterized by many spectroscopic and non-spectroscopic techniques to assess the suitability of the modified HAS process for component making as well as to evaluate the influence of  $\text{AlN}$  hydrolysis on the densification behaviour of  $\beta\text{-Si}_4\text{Al}_2\text{O}_2\text{N}_6$  precursor mixture.

## 2. Experimental procedure

### 2.1. Raw materials and powder processing

High purity  $\alpha\text{-Si}_3\text{N}_4$  (P95H, VESTA Ceramics AB, Sweden),  $\alpha\text{-Al}_2\text{O}_3$  (HP Grade, ACC India Ltd., India),  $\text{Y}_2\text{O}_3$  (Rhodia Inc., Phoenix, Arizona), and  $\text{AlN}$  (AT grade, HC Starck, GmbH, Germany) were used as starting raw materials. The surface treatment of as purchased  $\text{AlN}$  powder was performed according to the procedures reported in the literature to passivate its surface against hydrolysis.<sup>17–19</sup> The as-treated powder is hereafter termed as T- $\text{AlN}$ . In a typical experiment, precursor mixtures containing required quantities of  $\alpha\text{-Si}_3\text{N}_4$ , as-purchased  $\text{AlN}$  (A- $\text{AlN}$ ), surface treated  $\text{AlN}$  (T- $\text{AlN}$ ),  $\alpha\text{-Al}_2\text{O}_3$  and  $\text{Y}_2\text{O}_3$  (Table 1) were initially suspended in doubly distilled water to obtain aqueous slurries with 48–50 vol.% solids loading. To improve the dispersion of precursor mixtures and the fluidity of the suspension, Dolapix A88 (amino alcohol —cationic dispersant, Zschimmer & Schwarz, Berlin, Germany) was added in a ratio of 25  $\mu\text{l/g}$  of powder. All the slurries were degassed for  $\sim 5$  min after milling for 16 h by vacuum pumping. All the above operations were carried out at room temperature. Afterwards, the slurries were cast into non-porous white petroleum jelly coated split-type aluminium moulds ( $\sim 100/60$  mm  $\times$  30 mm  $\times$  30 mm), which were then allowed to set under ambient conditions for about 2 h followed by a stage at  $\sim 60^\circ\text{C}$  till the completion of the setting process. The green bodies thus obtained were de-moulded and

Table 1

Compositions of precursor  $\beta\text{-Si}_4\text{Al}_2\text{O}_2\text{N}_6$  mixtures required to prepare  $\sim 100$  cm<sup>3</sup> of 48 vol.% aqueous slurries to be consolidated by the modified hydrolysis-assisted solidification (HAS) process

Sample codes	Processing route	$\text{Al}_2\text{O}_3$ replaced by $\text{AlN}^{\text{a}}$ (%)	$\alpha\text{-Si}_3\text{N}_4$ (g)	A- $\text{AlN}$ (g)	H <sub>2</sub> O required to hydrolyze A- $\text{AlN}$ (g)	$\alpha\text{-Al}_2\text{O}_3$ (g)	$\text{Y}_2\text{O}_3$ (g)	T- $\text{AlN}^{\text{b}}$ (g)	H <sub>2</sub> O solvent (ml)	Dolapix A88 (ml)	Viscosity (MPa s)
HAS-5	HAS	5	107.87	6.88	4.64	30.53	12.26	15.79	47.70	4.33	94.09
HAS-10	HAS	10	107.87	13.77	9.29	21.77	12.26	15.79	47.91	4.28	271.5
HAS-15	HAS	15	107.87	20.66	13.95	13.01	12.26	15.79	48.05	4.23	391.4
HAS-22	HAS	22	107.87	30.89	20.85	—	12.26	15.79	48.17	4.17	105.6
CDPP <sup>c</sup>	CDPP	—	107.87	15.79	—	39.28	12.26	—	Pressed under 200 MPa load	—	—

<sup>a</sup> According to  $2\text{AlN} + 3\text{H}_2\text{O} \rightarrow \text{Al}_2\text{O}_3 + 2\text{NH}_3$ .

<sup>b</sup> A coating process developed by the authors was used to convert  $\text{AlN}$  into a hydrolysis resistant powder.

<sup>c</sup> Prior to pressing, this precursor mixture was mixed in a planetary ball mill for  $\sim 30$  min.

dried under controlled humidity (Model: LHL-113; Espec Corporation, Japan) conditions to avoid cracking.

For the sake of comparison, these materials were also prepared following a conventional dry-powder pressing (CDPP) route. In a typical experiment, ~200 g of a precursor mixture containing 64.33%  $\alpha$ - $\text{Si}_3\text{N}_4$ , 23.36%  $\alpha$ - $\text{Al}_2\text{O}_3$ , 9.37% A-AIN and 7%  $\text{Y}_2\text{O}_3$  was suspended in ~200 ml of toluene and mixed with ~60 g 5 wt.% aqueous PVA solution in a 500 ml of alumina bowl of a planetary ball mill (Retsch, Germany) in the presence of ~200 g of  $\text{ZrO}_2$  cylindrical pellets (10 mm diameter and 12 mm length) for ~30 min. The resultant dough was filtered off, dried at ~90 °C for 12 h in an electrically heated oven. The as-dried material was passed from –30 to +100 BSS mesh to make granules in the size range of 149–595  $\mu\text{m}$  prior to pressing into pellets having 30 mm diameter  $\times$  10 mm height under a pressure of 200 MPa. All the green samples were sintered at 1675 °C for 4 h in nitrogen atmosphere (>800 Torr). During sintering, the samples were covered with  $\text{Si}_3\text{N}_4$ –BN powder mixture (50%  $\text{Si}_3\text{N}_4$  and 50% BN) to protect them from decomposition and/or deformation.<sup>12</sup>

## 2.2. Materials characterization

Particle sizes of all the powders used were measured according to the Laser diffraction technique on particle size analyzer (Granulometer G 920, Cilas, France). The XRD patterns were recorded on a Bruker (Karlsruhe, Germany) D8 advanced system using a diffracted beam mono-chromated Cu K $\alpha$  (0.15418 nm) radiation source.<sup>20</sup> Crystalline phases were identified by comparison with PDF-4 reference data from International Centre for Diffraction Data (ICDD). Relative phase compositions of samples were calculated from the respective peaks' intensity. To obtain quantitative information of various phases, the most intense peak of the individual phases was taken into consideration.<sup>20</sup> The peak heights of all the phases were summed up and the percentage concentration of a particular phase was estimated from the ratio of the strongest peak of that phase to the sum of various phases present in a given system.<sup>20</sup>

The absolute viscosity of particulate slurries was measured using a piston type viscometer (Viscolab 4100, Cambridge Applied Systems Inc., MA).<sup>21</sup> The coefficient of thermal expansion (CTE) of sintered samples was measured with a Netzsch 402C dilatometer in the temperature range of 30–700 °C. Bulk density (BD), apparent porosity (AP), and water absorption (WA) capacity of various sintered materials was measured according to Archimedes principle (ASTM C372) using Mettler balance and the attachment (AG 245, Mettler Toledo, Switzerland). On average, three measurements were performed on each sample in this study. The microstructure of dense  $\beta$ -SiAlON ceramics was examined using scanning electron microscope (Hitachi, S-3400N, Scanning Electron Microscope, Japan). The fracture toughness values ( $K_{\text{Ic}}$ ) were determined on the basis of the indentation method [ $K_{\text{Ic}} = Ha^{1/2} \times 0.203 (C/a)^{-3/2}$ ].<sup>22</sup> Here,  $2a$  represents Vickers indent diagonal length,  $2C$  the resulting crack length and  $H$  is a Vickers hardness ( $Hv = \text{kg}/\text{mm}^2 = 10 \text{ MPa}$ ). The required

hardness, crack and diagonal length data was collected using a micro-hardness tester (Leitz Wetzler, Germany) by holding the indenter tip (137°) under a load of 2 kg for 20 s on the surface of the sample having mirror finish. Five to six samples were examined per case in order to check the reproducibility of results and all the readings were averaged out.

## 3. Results and discussion

Normally to synthesize advanced materials such as, dense SiAlON ceramics with tailored properties, the use of suitable starting raw materials is very important as the consolidation and densification process is highly influenced by their purity, average particle sizes, and particle size distributions. Further, the morphology of the particles and the state of powder agglomeration play key roles in the case of colloidal processing techniques, determining the maximum achievable solids loading. This particularly crucial in the case of new shaping techniques in which consolidation takes place without liquid removal and the minimisation of the shrinkage demands slurries with solids loadings of at least ~50 vol.%.<sup>23</sup> The particle size distributions and the morphological features of the starting raw materials used in this study are presented in Figs. 1 and 2, respectively. Fig. 1 shows that the yttria and alumina powders have uni-modal and narrow particle size distributions, whereas the nitride powders have relatively wider particle size distributions, especially the silicon nitride with an average particle/agglomerate size of ~18  $\mu\text{m}$ . Fig. 2 reveals that the presence of hard agglomerates is a common feature among all the powders, certainly derived from their preparation history. The SEM micrographs show that the primary particles of A-AIN and  $\alpha$ - $\text{Al}_2\text{O}_3$  are more regular in shape in comparison to those of  $\alpha$ - $\text{Si}_3\text{N}_4$  and  $\text{Y}_2\text{O}_3$  powders.

The various precursor mixtures and the viscosity values of the slurries used in this study are given in Table 1. As can be seen, all the slurries exhibits reasonably low viscosity values to be cast and to obtain defect free green parts.<sup>22</sup> In general, for slurries containing both  $\text{Al}_2\text{O}_3$  and A-AIN powders, the viscosity increases with the content of A-AIN. The changes in viscosity and temperature occurred in a 49 vol.% solids slurry of the HAS-

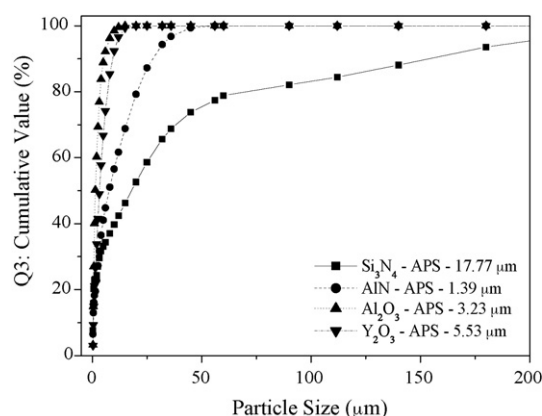


Fig. 1. Particle size distribution of the as-received raw materials used in this study.

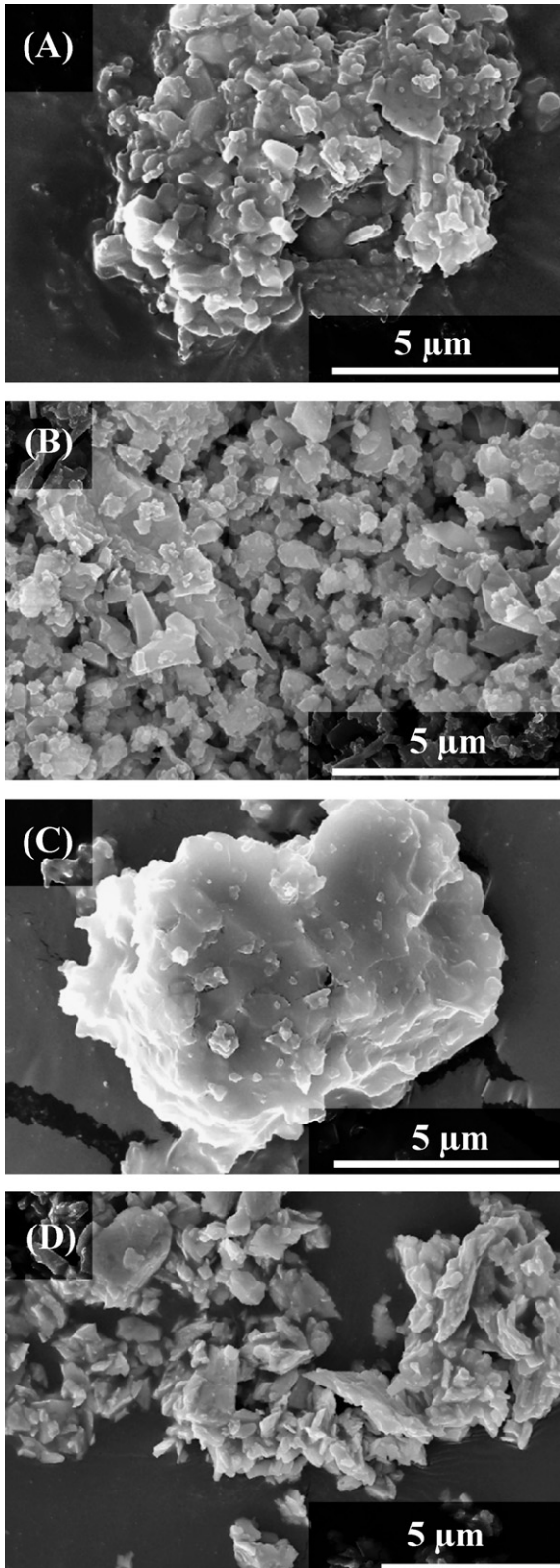


Fig. 2. SEM micrographs of the as-received powders: (A)  $\alpha$ - $\text{Al}_2\text{O}_3$ , (B)  $\alpha$ - $\text{Si}_3\text{N}_4$ , (C) AlN, and (D)  $\text{Y}_2\text{O}_3$ .

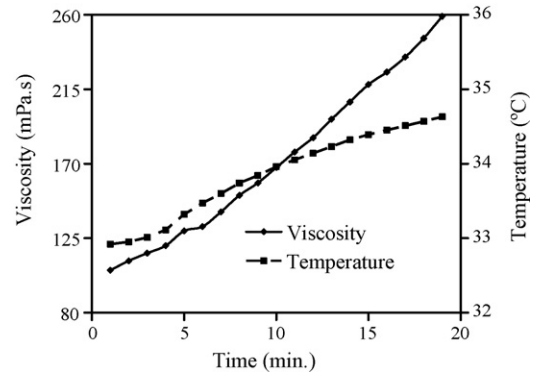


Fig. 3. Viscosity and temperature variations of the HAS-5 slurry containing 49 vol.% solids as function of time as-measured in a piston type viscometer.

5 composition were monitored along a period of about 20 min in a piston type viscometer to access the effects of hydrolysis time on the slurry characteristics. The resultant data plotted in Fig. 3 clearly indicate that the as-purchased AlN powder undergoes continuous hydrolysis leading to increases in both the temperature and the viscosity of the slurry, which are according to the findings reported elsewhere.<sup>24</sup>

The properties of sintered  $\beta$ - $\text{Si}_4\text{Al}_2\text{O}_2\text{N}_6$  materials obtained by both HAS and CDPP consolidation processes are presented in Table 2 along with their corresponding green density (GD) data. The CDPP sample exhibits a slightly higher GD in comparison to the samples consolidated by HAS (HAS-5 and HAS-10). The HAS-15 and HAS-22 samples were found to have a lot of internal porosity. After overnight treating at 60 °C they looked like foams. However, when these samples were allowed to set under ambient conditions, they exhibited an exceptionally high strength after overnight drying at >70 °C, although some internal pores in the range of 500–1000  $\mu\text{m}$  diameter have been developed. The green microstructures of HAS-5 and HAS-10 samples were found to be almost similar to that of CDPP sample even after setting overnight at 60 °C. Defect free rectangular bars with 90 mm  $\times$  55 mm  $\times$  25 mm size were successfully consolidated by HAS process from the slurry containing 50 vol.% HAS-5 precursor mixture.

As can be seen from sintered properties (Table 2), in general, both HAS-5 and CDPP samples exhibit almost similar

Table 2  
Properties of various  $\beta$ - $\text{Si}_4\text{Al}_2\text{O}_2\text{N}_6$  ceramics sintered at 1675 °C for 4 h<sup>a</sup>

Property	CDPP	HAS-5	HAS-10	HAS-15 <sup>b</sup>	HAS-22 <sup>b</sup>
GD <sup>c</sup> (g/cm <sup>3</sup> )	1.871	1.73	1.78	–	–
BD (g/cm <sup>3</sup> )	3.067	3.12	2.91	3.14	3.01
AP (%)	0.012	0.47	0.05	0.07	0.89
WA (%) capacity	0.004	0.16	0.01	0.02	0.298
$\beta$ -SiAlON phase	94.43	~94	~90	~80	~43
Linear shrinkage (%)	14	17	15.75	14.66	14.43

GD, green density; BD, bulk density; AP, apparent porosity; WA, water absorption.

<sup>a</sup> The slurries of HAS-5 to HAS-22 compositions had 48 vol.% solids.

<sup>b</sup> BD, AP and WA were measured in tiny (ca. 2–3 mm sized) samples.

<sup>c</sup> The HAS samples were set overnight at 60 °C.

values of BD, AP and WA, whereas the samples from HAS-10 to HAS-22 show relatively inferior properties. The values of BD, AP and WA capacity reported in Table 2 are not representative of the whole  $\sim 90 \text{ mm} \times 28 \text{ mm} \times 25 \text{ mm}$  rectangular samples but for tiny ground parts of about 2–3 mm in size. A similar BD of  $3.02 \text{ g/cm}^3$  was also reported for the same  $\beta\text{-Si}_4\text{Al}_2\text{O}_2\text{N}_6$  composition consolidated by aqueous gelcasting.<sup>10,11</sup> Interestingly, both CDPP and HAS-5 samples exhibit values of BD  $>3.02 \text{ g/cm}^3$  and of AP and WA capacity  $<0.2$  and  $<0.6\%$ , respectively. The linear shrinkage values associated with the drying and sintering steps of HAS-5 sample obtained from a slurry with 48 vol.% solids loading were found to be  $\sim 2$  and  $\sim 15\%$ , respectively (total linear shrinkage of  $\sim 17\%$ ). The CDPP sample exhibited a linear shrinkage of  $\sim 14\%$ . However, the highest value of BD was measured for the tiny samples broken from the HAS-15 body, with similar microstructure being observed for the HAS-22 body. This means that the overall lower sintered density values of these samples derived only from the internal porosity left upon consolidation, since these compositions exhibited improved sintering ability.<sup>25</sup> It is a well-known fact that powders with fine particle sizes and narrow particle size distributions exhibit faster sintering kinetics. During reactive formation of  $\beta\text{-Si}_4\text{Al}_2\text{O}_2\text{N}_6$  in the absence of sintering aids, a rapid phase formation takes place at about  $1600^\circ\text{C}$  due to the existence of eutectic temperature at  $1587^\circ\text{C}$  between  $\text{Al}_2\text{O}_3$  and  $\text{SiO}_2$  (present on the surface of  $\text{Si}_3\text{N}_4$  due to surface oxidation that is difficult to avoid). This rapid phase formation leads to limited grain boundary phase and hence, to a limited densification and a relatively high fraction of remaining porosity.<sup>26,27</sup> However, in the presence of  $\text{Y}_2\text{O}_3$ , an eutectic point forms in the system  $\text{Y}_2\text{O}_3\text{-Al}_2\text{O}_3\text{-SiO}_2$  at  $1350^\circ\text{C}$ . As this temperature is much lower than the on-set temperature at which  $\beta\text{-SiAlON}$  phase formation starts (i.e.,  $\sim 1600^\circ\text{C}$ ), a glassy phase is easily formed during sintering and contributes to densification through enhanced particle rearrangement. This is the probable reason for the high bulk sintered densities observed for the HAS-5 and CDPP  $\beta\text{-Si}_4\text{Al}_2\text{O}_2\text{N}_6$  materials.

The X-ray diffraction patterns of HAS-5 and CPDD samples sintered at  $1675^\circ\text{C}$  for 4 h are presented in Fig. 4. As can be seen from this figure, both materials exhibited XRD patterns primarily due to  $\beta\text{-SiAlON}$  phase ( $\beta\text{-Si}_4\text{Al}_2\text{O}_2\text{N}_6$ , ICDD File No.: 00-048-1616). Very interestingly, none of the samples show XRD lines corresponding to their starting raw materials, i.e.,  $\alpha\text{-Si}_3\text{N}_4$ ,  $\alpha\text{-Al}_2\text{O}_3$ , AlN and  $\text{Y}_2\text{O}_3$ , confirming the formation of  $\beta\text{-SiAlON}$  phase upon reactive sintering at  $1675^\circ\text{C}$  for 4 h. Few minor XRD lines in addition to  $\beta\text{-SiAlON}$  phase are also manifested in both the spectra, which are ascribed to  $\text{Y}_2\text{SiAlO}_5\text{N}$  phase (ICDD File No.: 00-048-1627). The HAS-15 and HAS-22 samples exhibited only  $\sim 80$  and  $\sim 43\%$  of  $\beta\text{-SiAlON}$  phase after sintering at  $1675^\circ\text{C}$  for 4 h, respectively (Table 2), with remaining phases of AlN,  $\text{Al}_2\text{O}_3$  and  $\text{Si}_3\text{N}_4$ . These results suggest that even though the required amount of water was available in the slurry at the time of casting (Table 1), this water was not sufficient to hydrolyze the total bare AlN powder in the HAS-22 precursor mixture as part of this water evaporated during setting at  $60^\circ\text{C}$  before complete

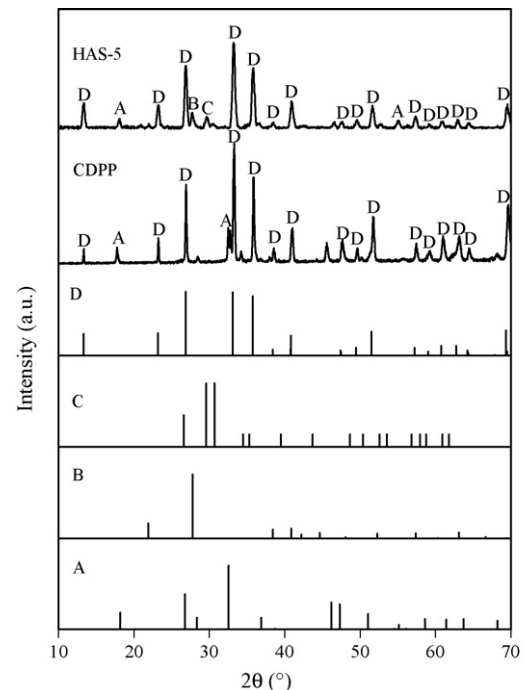


Fig. 4. XRD patterns of sintered ( $1675^\circ\text{C}$  for 4 h)  $\beta\text{-Si}_4\text{Al}_2\text{O}_2\text{N}_6$  ceramics consolidated by hydrolysis-assisted solidification from a slurry containing 48 vol.% solids of the HAS-5 composition, and by the conventional dry-powder pressing (CDPP) route: (A)  $\text{Y}_2\text{SiAlO}_5\text{N}$ , ICDD File No.: 00-48-1627; (B) crystalline  $\text{SiO}_2$ , ICDD File No.: 01-085-0462; (C)  $\text{YO}_{1.335}$ , ICDD File No.: 00-039-1065; (D)  $\text{Si}_4\text{Al}_2\text{O}_2\text{N}_6$ , ICDD File No.: 00-48-1616.

hydrolysis of AlN powder. This could be the most probable reason for low degree of transformation into  $\beta\text{-SiAlON}$  phase in the case of HAS-22 upon reaction sintering at  $1675^\circ\text{C}$  for 4 h under 800 Torr  $\text{N}_2$  pressure. The sintered data available in Table 2 further suggests that the phase formation and densification occur independently upon reaction sintering at elevated temperatures.

In order to understand the effect of solids loading on the shape making capability as well as on the sintering behaviour, suspensions of the HAS-5 precursor mixture were also prepared with 49 and 50 vol.% solids, cast and consolidated by the HAS process, and sintered at  $1675^\circ\text{C}$  for 4 h (Table 3). As can be seen, the increase in the solids loading has also increased the viscosity of the slurry to some extent and led to a slight decrease in

Table 3  
Properties of sintered ( $1675^\circ\text{C}$  for 4 h)  $\beta\text{-Si}_4\text{Al}_2\text{O}_2\text{N}_6$  ceramics consolidated from slurries with different loadings of the precursor mixture HAS-5

Property	48 vol.%	49 vol.%	50 vol.%
Viscosity (MPa s)	94.09	111.3	299.6
GD ( $\text{g/cm}^3$ )	1.73	1.65	1.68
BD ( $\text{g/cm}^3$ )	3.12	3.15	3.32
AP (%)	0.47	0	0
WA (%) capacity	0.16	0	0
$\beta\text{-SiAlON}$ phase	$>93\%$	$>93\%$	$>93\%$
Linear shrinkage (%)	17	15	14
Hardness ( $\text{kg/mm}^2$ )	$1571 \pm 6$	$1553 \pm 4$	$1590 \pm 5$
Fracture toughness ( $\text{MPa m}^{1/2}$ )	$3.42 \pm 0.4$	$3.48 \pm 0.2$	$3.39 \pm 0.3$

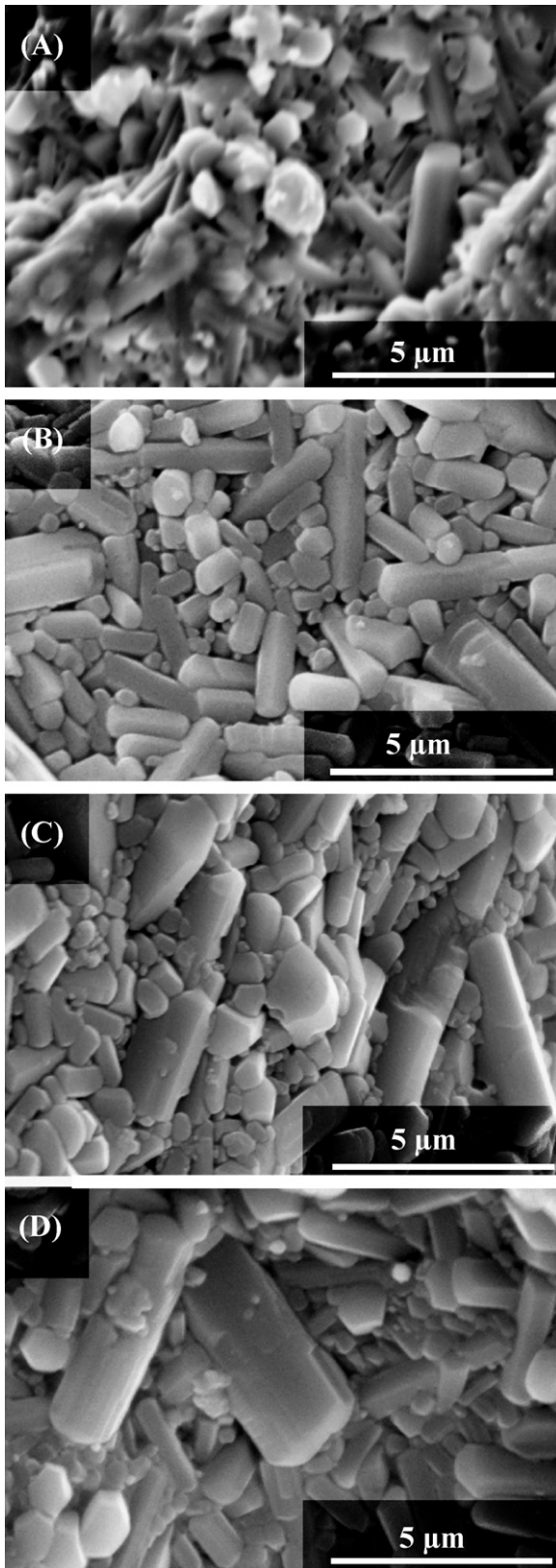


Fig. 5. SEM micrographs of sintered (1675 °C for 4 h)  $\beta$ - $\text{Si}_4\text{Al}_2\text{O}_2\text{N}_6$  ceramics derived from (A) CDPP sample; and from HAS-5 sample consolidated by HAS from slurries containing different solids loading: (B) 48 vol.%; (C) 49 vol.%, and (D) 50 vol.%.

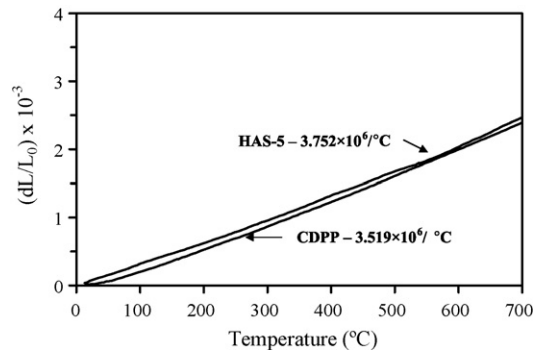


Fig. 6. CTE of the sintered (1675 °C for 4 h)  $\beta$ - $\text{Si}_4\text{Al}_2\text{O}_2\text{N}_6$  ceramics consolidated from a slurry containing 48 vol.% solids of the HAS-5 composition.

the GD of the cast parts. However, it had a small positive effect on the sintered bulk density, probably due to a hindering particle segregation effect, while the values of AP and WA capacity were reduced to zero. As expected, the solids loading also had a positive effect on total linear shrinkage of the samples. The sample with 48 vol.% solids experienced a higher linear shrinkage (17%) in comparison to the one with 50 vol.% solids (14%). The measured hardness (1571–1590 Hv) and fracture toughness (3.419–3.19  $\text{MPa m}^{1/2}$ ) values are typical of  $\beta$ - $\text{SiAlON}$ .<sup>28</sup> Both properties were only slightly dependent on solids loading.<sup>28</sup> The mechanical properties of the materials consolidated by the modified HAS process were found to be superior than those of the CPDD sample (1317 Hv and 3.30  $\text{MPa m}^{1/2}$ ), but the phase formation has shown to be insensitive to the consolidation method employed.

The SEM micrographs of sintered (1675 °C for 4 h) HAS-5 samples obtained from slurries containing 48, 49 and 50 vol.% solids and by CDPP are presented in Fig. 5. A close look at these micrographs reveals that the microstructures of the HAS samples look like more homogeneous than that of CDPP sample. This last sample also seems to be more porous in comparison to others, what is in good agreement with the AP and WA values reported in Tables 2 and 3. Different factors might contribute to the observed differences. The first one is the higher degree of homogeneity achieved in the slurry state, which is then preserved during the consolidation process. Another one is the uniform distribution of fine and high reactive  $\text{Al}(\text{OH})_3$  layer formed around the  $\text{AlN}$  particles due to hydrolysis, which can easily react with the other powder particles, facilitating the sintering process.<sup>14,15</sup>

The thermal behaviour of  $\beta$ - $\text{Si}_4\text{Al}_2\text{O}_2\text{N}_6$  materials is of paramount importance. Fig. 6 compares the dilatometric curves in the range of 30–700 °C of CDPP and HAS-5 samples sintered at 1675 °C for 4 h. Both exhibit comparable values of CTE within the temperature range tested ( $3.52 \times 10^{-6} \text{ }^\circ\text{C}^{-1}$  for CPDD and  $3.75 \times 10^{-6} \text{ }^\circ\text{C}^{-1}$  for HAS-5). The reason for the slightly higher CTE exhibited of the HAS-5 sample as compared to its counterpart CDPP is certainly related to the observed micro-structural differences. A close CTE value of  $4.1 \times 10^{-6} \text{ }^\circ\text{C}^{-1}$  between 25 and 1000 °C was also reported for  $\beta$ - $\text{Si}_4\text{Al}_2\text{O}_2\text{N}_6$  consolidated by gelcasting.<sup>10,11</sup> Thus, the CTE values observed in the present study compare well with the reported results.

#### 4. Conclusions

The following conclusions can be drawn from the above study:

- (1) Dense  $\beta$ -Si<sub>4</sub>Al<sub>2</sub>O<sub>2</sub>N<sub>6</sub> ceramics with a theoretical density of more than 98% could be prepared by a modified hydrolysis-assisted solidification (HAS) technique in which only the unprotected AlN plays a role in the consolidation process.
- (2) Defect free sintered  $\beta$ -Si<sub>4</sub>Al<sub>2</sub>O<sub>2</sub>N<sub>6</sub> rectangular bars with dimensions of 90 mm × 55 mm × 25 mm could be fabricated by the modified HAS route upon replacing 5–10 wt.% alumina by unprotected AlN powder.
- (3)  $\beta$ -Si<sub>4</sub>Al<sub>2</sub>O<sub>2</sub>N<sub>6</sub> ceramics consolidated by the modified HAS route from slurries containing 49–50 vol.% of the HAS-5 precursor mixture in which 5 wt.% Al<sub>2</sub>O<sub>3</sub> was replaced by an equivalent amount of unprotected AlN powder, exhibit superior properties (BD ~3.15–3.32 g/cm<sup>3</sup>, AP and WA of 0.0%, contents of  $\beta$ -SiAlON >93%, hardness values of 1553–1590 kg/mm<sup>2</sup> and fracture toughness >3.40 MPa m<sup>1/2</sup>) in comparison to  $\beta$ -Si<sub>4</sub>Al<sub>2</sub>O<sub>2</sub>N<sub>6</sub> ceramics consolidated by the conventional dry-powder pressing.

#### Acknowledgements

IG thanks SERC-DST (Government of India) for awarding BOYSCAST fellowship (SR/BY/E-04/06). Thanks are also due to CICECO for the financial support.

#### References

1. Oyama, Y. and Kamagaito, O., Solid solubility of some oxides in Si<sub>3</sub>N<sub>4</sub>. *Jpn. J. Appl. Phys.*, 1971, **10**, 1637–1642.
2. Jack, K. H. and Wilson, W. I., Ceramics based on the Si–Al–O–N and related systems. *Nat. (Lond.) Phys. Sci.*, 1977, **238**, 28–29.
3. Jack, K. H., Review: SiAlONs and related nitrogen ceramics. *J. Mater. Sci.*, 1976, **11**, 1135–1158.
4. Jack, K. H., In *SiAlONs A Study in Materials Development, Non-oxide Technical and Engineering Ceramics* ed. Stuart Hampshire, Elsevier Applied Science Publishers Ltd., Barking, Essex, England, 1986, 1–30.
5. Brown, I. W. M., Barris, G. C., Bowden, M. E., Mackenzie, K. J. D., Shepard, C. M. and White, G. V., Synthesis, densification, and properties of SiAlON bodies and composites, in a Book entitled “SiAlONs”. In *Key Engineering Materials*, ed. K. Komeya, M. Mitomo and Y. B. Cheng. Trans Tech Publications Ltd., USA, 2001.
6. Demit, J., Method of manufacturing  $\beta$ -SiAlON ceramics, US Patent 4,147,759, April 3; 1979.
7. Lumby, R.J., Wills, R.R., and Horsley, R.F., Method of forming ceramic products, US Patent 3,991,148; November 9, 1976.
8. Xu, X., Marta, I. L. L., Oliveira, R. F. and Ferreira, J. M. F., Effect of dispersant on the rheological properties and slip casting of concentrated SiAlON precursor suspensions. *J. Eur. Ceram. Soc.*, 2003, **23**(9), 1525–1530.
9. Acikbas, N. C., Suvaci, E. and Mandal, H., Fabrication of functionally graded SiAlON ceramics by tape casting. *J. Am. Ceram. Soc.*, 2006, **89**(10), 3255–3257.
10. Kirby, K. W., Jankiewicz, A., Kupp, D., Walls, C. and Janney, M., Gelcasting of ceramic radomes in the Si<sub>3</sub>N<sub>4</sub>–Al<sub>2</sub>O<sub>3</sub>–AlN–SiO<sub>2</sub> system. *Mater. Tech. Adv. Perf. Mater.*, 2001, **16**(3), 187–190.
11. Janney, M. A., Walls, C. A., Kupp, D. M. and Kirby, K. W., Gelcasting SiAlON radomes. *Am. Ceram. Soc. Bull.*, 2004, 9201–9206.
12. Xu, X. and Ferreira, J. M. F., Temperature-induced gelation of concentrated SiAlON suspensions. *J. Am. Ceram. Soc.*, 2005, **88**(3), 593–598.
13. Kosmac, T., Novak, S. and Sajko, M., Hydrolysis-assisted solidification (HAS): a new setting concept for ceramic net-shaping. *J. Eur. Ceram. Soc.*, 1997, **17**, 427–432.
14. Novak, S., Kosmac, T., Krnel, K. and Draz, G., Principles of the hydrolysis assisted solidification (HAS) process for forming ceramic bodies from aqueous suspension. *J. Eur. Ceram. Soc.*, 2002, **22**, 289–295.
15. Li, W., Liu, Z., Gu, M. and Jin, Y., Hydrolysis assisted solidification of silicon carbide ceramics from aqueous suspension. *Ceram. Int.*, 2005, **31**, 159–163.
16. Janney, M. A., Nunn, S. D., Walls, C. A., Omatete, O. O., Ogle, R. B., Kirby, G. H. and McMillan, A. D., Gelcasting. In *The Handbook of Ceramic Engineering*, ed. M. N. Rahman. Marcel Dekker, New York, 1998, pp. 1–15.
17. Uenishi, F. M., Hashizume, K. N. Y., and Yokote, T., Aluminum nitride powder having improved water resistance, US Patent No. 4,923,689; May 8, 1990.
18. Krnel, K. and Kosmac, T., Protection of AlN powder against hydrolysis using aluminum di-hydrogen phosphate. *J. Eur. Ceram. Soc.*, 2001, **21**, 2075–2079.
19. Olhero, S. M., Novak, S., Oliveira, M., Krnel, K., Kosmac, T. and Ferreira, J. M. F., A thermo-chemical surface treatment of AlN powder for the aqueous processing of AlN ceramics. *J. Mater. Res.*, 2004, **19**(3), 746–751.
20. Klug, M. P. and Alexander, L. E., *X-ray Diffraction Procedure for Polycrystalline and Amorphous Materials*. Wiley, New York, 1974, p. 634.
21. Ganesh, I., Jana, D. C., Shaik, S. and Thiagarajan, N., An aqueous gelcasting process for sintered silicon carbide ceramics. *J. Am. Ceram. Soc.*, 2006, **89**(10), 3056–3064.
22. Ekberg, I.-L., Lundberg, R., Warren, R. and Carlson, R., *British Matrix Composites*, 2, ed. A. M. Brandt and I. H. Marshall. Elsevier Applied Science, 1998.
23. Lyckfeldt, O. and Ferreira, J. M. F., Processing of porous ceramics by starch consolidation. *J. Eur. Ceram. Soc.*, 1998, **18**(2), 131–140.
24. Oliveira, M., Olhero, S., Rocha, J. and Ferreira, J. M. F., Controlling hydrolysis and dispersing AlN powders in aqueous media. *J. Colloid Interf. Sci.*, 2003, **261**, 456–463.
25. Kudyba-Jansen, A. A., Hintzen, H. T. and Metselaar, R., The influence of green processing on the sintering and mechanical properties of  $\beta$ -SiAlON. *J. Eur. Ceram. Soc.*, 2001, **21**(12), 2153–2160.
26. Hampshire, S., Park, H. K., Thompson, D. P. and Jack, H. K.,  $\alpha'$ -SiAlON. *Nat. (Lond.)*, 1978, **274**, 880–882.
27. Yang, J. F., Zhang, G. J., She, J. H., Ohji, T. and Kanzaki, S., Improvement of mechanical properties and corrosion resistance of porous  $\beta$ -SiAlON ceramics by low Y<sub>2</sub>O<sub>3</sub> additions. *J. Am. Ceram. Soc.*, 2004, **87**(9), 1714–1719.
28. Pettersson, P., Shen, Z., Johnson, M. and Nygren, M., Thermal shock properties of  $\beta$ -SiAlON ceramics. *J. Eur. Ceram. Soc.*, 2002, **22**, 1357–1365.